Driving self-sustained vibrations of nanowires with a constant electron beam

P. Vincent,[1,*] S. Perisanu,[1] A. Ayari,[1] M. Choueib,[1,2] V. Gouttenoire,[1] M. Bechelany,[2] A. Brioude,[2] D. Cornu,[2] and S. T. Purcell[1]

[1]*Université de Lyon, F-69000, France and Université Lyon 1, Laboratoire PMCN, CNRS, UMR 5586, F69622 Villeurbanne Cedex, France*

[2]*Laboratoire Multimatériaux et Interfaces, Université Lyon 1, CNRS, UMR 5615, Domaine Scientifique de la Doua, F-69622 Villeurbanne Cedex, France*

(Received 15 March 2007; published 30 August 2007)

We present a method for driving self-sustained mechanical oscillations of nanocantilevers, in the form of SiC nanowires, using the constant electron beam of a scanning electron microscope. A model is developed incorporating the electrical and mechanical system elements and the physics of electron beam interactions with an insulator. Energy is pumped into the oscillations by the beam-induced time-varying charge on the nanowire coupled to the system capacitance. This self-sustained excitation method and its accompanying model provide a tool for nanoelectromechanical systems.

DOI: 10.1103/PhysRevB.76.085435 PACS number(s): 85.85.+j, 62.25.+g, 62.40.+i

Nanoelectromechanical systems (NEMS) in which the active element is a resonating nanocantilever are receiving increasing attention from the nanoscience research community for a wide range of technological and basic research ideas, and as a materials characterization tool for nanotubes and nanowires. The basic elements of a NEMS are (1) excitation, (2) mechanical resonator, (3) perturbation to be measured, and (4) detection.[1] Resonator excitation is currently realized by electrostatic forces, Lorentz forces, and optothermal effects, all of which have their advantages and limitations.[1] New excitation and detection strategies for NEMS may be the key to unlocking applications such as quantum macroscopic oscillations[2] or single molecule detection[3] which depend on mastering ever smaller cantilevers, vibration amplitudes, and signal-to-noise ratios. Self-oscillation is a nonintuitive but fairly common phenomena where a constant driving force excites the natural resonances of a system. Examples are the shimmy in an automobile, the famous Tacoma Narrows Bridge oscillation, the note from a human voice, and even a Bronx cheer. Closer to our interests is the recent laser excitation of self-sustained oscillations of nanocantilevers within an interferometer arrangement.[4] Strategies that combine self-sustained oscillations with new excitation and detection methods may prove useful or necessary to achieve ultimate measurement limits.

In this paper we first show that under the right conditions the constant electron beam of a scanning electron microscope (SEM) can be used to excite self-sustained mechanical oscillations of nanowires. These oscillations are at the fundamental mode frequency of the nanowire $\nu_0=\omega_0/2\pi$. Second we develop a model that proves that the source of the oscillations is the beam-induced time-varying charge on the nanowire coupled to the system capacitance. The model takes into account the beam charging, *RC* decharging, and the electrostatic, elastic, and dissipative forces. Simulations are carried out with the two coupled differential equations that describe the phenomenon and the parameters of the studied nanowire. These follow the oscillation behavior semiquantitatively. Finally an analytical analysis is made which allows us to understand this model NEMS system and to predict its behavior for a larger set of physical parameters.

The nanowires studied in this work are large gap semiconducting SiC nanowires. They are high quality single crystals grown in mass by a patented high temperature vapor-solid technique.[5] Individual nanowires are glued by a conductive carbon tape to the apexes of etched tungsten tips [Fig. 1(a)] and introduced into the SEM. The SEM was equipped with a three-dimensional (3D) movement that allowed the maneuvering of an additional electrode in the vicinity of the nanowire. Before studying the self-sustained oscillations, the mechanical properties of the nanowires were determined by a variety of methods. The mechanical resonances were excited by small amplitude electrostatic sinusoidal voltages from a function generator and observed in the normal image mode permitting the determination of the Young's modulus *E*.[6] The SEM was used in line scan mode to determine the frequency dependant amplitude and thus the quality factor *Q*, and in spot mode (see below) to differentiate between the natural and parametric resonances.[7] For the nanowire in Fig. 1(a) we obtained $E=470$ GPa and a $Q=5000$. (Note: *Q* can reach 159 000 in ultrahigh vacuum for these SiC nanowires.[8])

In spot mode the scanning is turned off resulting in a focused beam that can be precisely positioned with respect to the nanowire [Figs. 1(a) and 1(b)], i.e., with respect to the SEM image. When a vibrating nanowire passes the focus, the resulting secondary electron burst generates a peak in the scintillator. This signal is captured with an oscilloscope and thus measures the real oscillation period [Fig. 1(c)]. The intensity of this peak is proportional to the illumination time. The highest signal occurs when the spot is focused at the oscillation maximum because the velocity reaches zero. For other positions two smaller peaks are observed since the nanowire crosses the electron beam twice per period [Figs. 1(b) and 1(c), position 2]. The signal and noise is weaker when approaching the equilibrium position where the velocity is highest.

The central experimental fact in this paper is that the nanowire can oscillate in spot mode with no ac or dc driving voltage applied to the electrode. When the beam is focused at the nonvibrating nanowire extremity [Fig. 1(a), position 3a], the oscilloscope signal then spontaneously presents the same

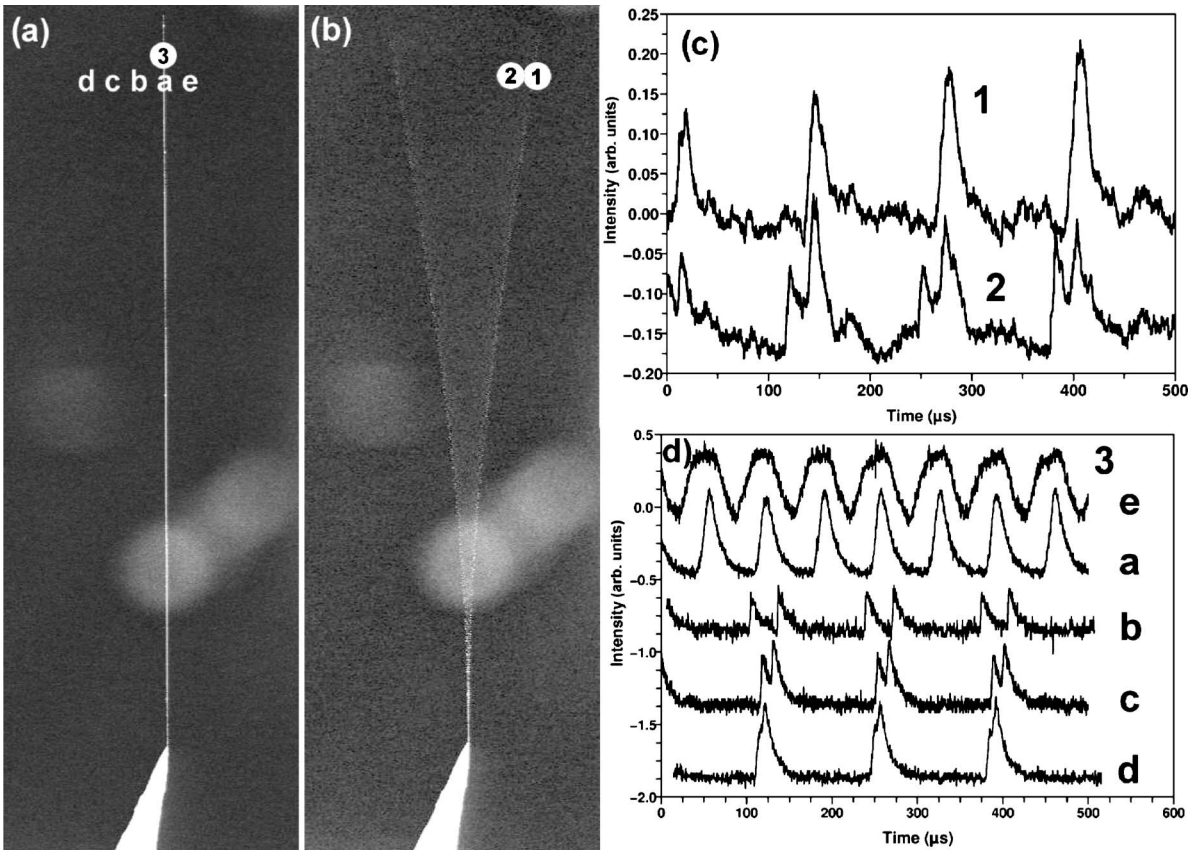

FIG. 1. (a) SiC nanowire (L=243 μm, ϕ=270 nm) mounted on a tungsten tip. (b) First vibration mode excited by an ac voltage at 7700 Hz. (c) Spot mode scintillator signals recorded on the oscilloscope for (b). Curve 1 is for the spot positioned at the amplitude extremum. The period gives the vibration frequency. Curve 2 is for the spot displaced into the oscillation. The peak splits into two smaller peaks. (d) Signals obtained without any ac excitation for different lateral spot positions. The signal period is twice the resonance period except for the extremum position d.

general shape as during the electrostatically excited oscillations. The peak repeats at double the fundamental frequency because the nanowire passes twice through the beam [Fig. 1(d) position a]. When the SEM is switched back to image mode the oscillation of the nanowire can be seen briefly before dropping to zero amplitude in a time $\approx Q/\nu_0$. More information is obtained by displacing the beam laterally with respect to the now oscillating nanowire [a,b,c,d,e in Figs. 1(a) and 1(d)]. Define x_b as the beam position with x_b=0 the nanowire rest position. The oscillations persist to maximum beam displacements on either side (d,e) after which they disappear. The displacement at d is much larger than at e, i.e., the response is very asymmetric. The obvious conclusion is that the electron beam provides energy to the nanowire to induce self-sustained oscillations. Simple calculations allowed us to immediately discard the direct transfer of beam momentum as the source of oscillations. The asymmetry leads us to consider the essential role of the electrical capacitance of the nanowire environment.

The cycle of charge injection and charge depletion as the nanowire enters and exits the electron beam is modeled next to explain the excitation and asymmetry. The nanowire is a mechanical resonator with effective spring constant k and mass m^*. k and m^* are given by $k=3EI/L^3$, I the geometrical inertial moment, L the length, and $m^*=0.2455\times$ (total nanowire mass). The nanowire is also an RC circuit element with R being the resistance of the nanowire and C the capacitance between the nanowire extremity and its environment. This capacitance leads to a cyclic electrostatic force which increases as the charge q at the nanowire extremity builds up and diminishes as q decreases by RC relaxation.

The equation of motion of the nanowire extremity is

$$m^*\ddot{x} + \frac{\omega_0 m^*}{Q}\dot{x} + kx = F(q), \tag{1}$$

where $F(q)$ is the net force induced by the charge q.

The charging is caused by the focused electron beam (current i_b=100 pA measured by a Faraday cup, energy 20 kV) and is localized at the nanowire apex. For this electron energy the penetration depth calculated from the Kanaya-Okayama equation[9] is 3.3 μm, much larger than the nanowire diameter. Thus essentially all primary electrons pass through the nanowire and a positive charging occurs due to secondary electron emission $\equiv\delta(q)i_b$. The charging fraction $\delta(q)$ is dependent on q because the positive charge on the insulating SiC increases the potential and eventually blocks the emission of secondary electrons. $\delta(q)=0$ is a steady state characterized by a quasistatic charge Q_{max}. Thome *et al.*[10] measured an exponential dependence in time when irradiat-

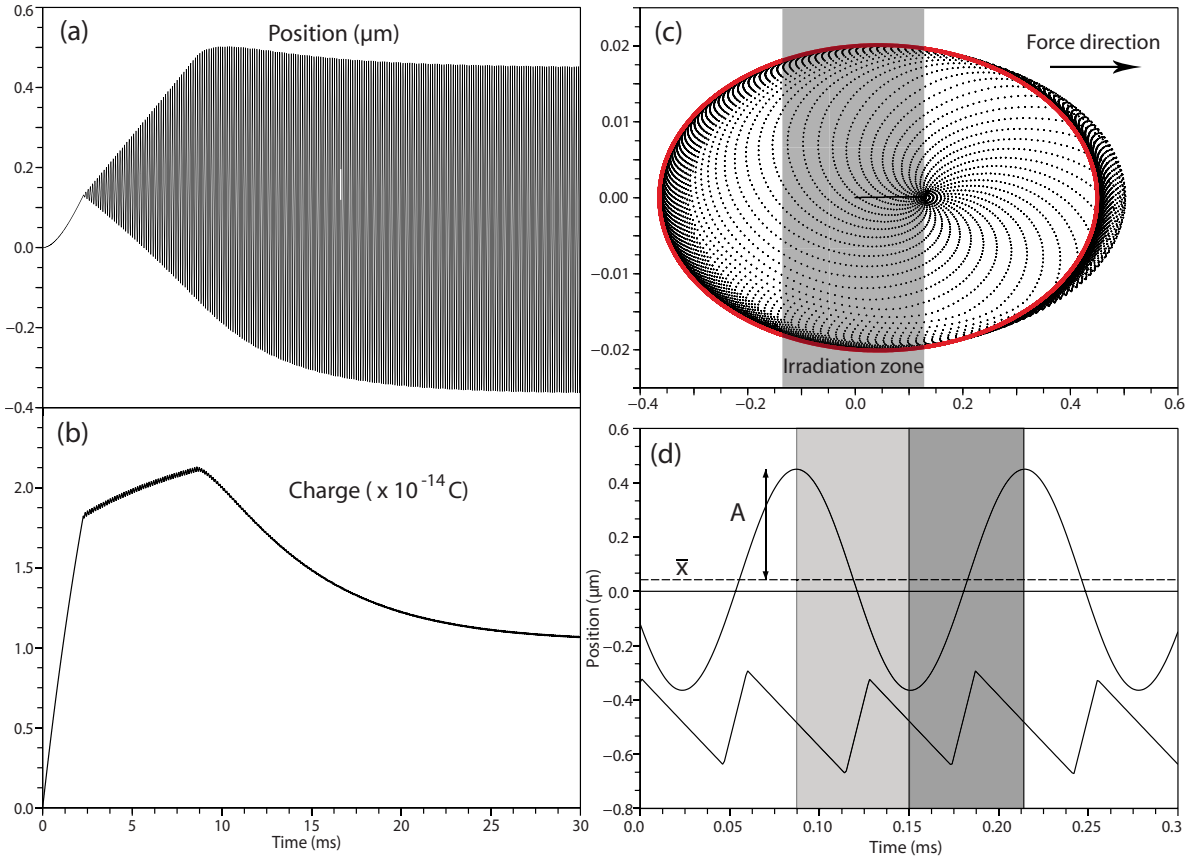

FIG. 2. (Color online) (a) and (b) Simulation of the nanowire position and charge when the beam is focused on the nanowire showing the self-sustained oscillations. (c) Phase plane representation of the motion in (a). Note the apparition of the limit cycle. The irradiation zone is represented in gray. A peak is detected each time the nanowire crosses this zone. (d) Detail of the nanowire motion when the limit cycle is reached. The dark gray represents the interval where $F(q)$ adds energy and the light gray where it removes energy (see text).

ing an insulator which can be written as $\delta(q)=\delta_0\left(1-\frac{q}{Q_{max}}\right)$. Note that δ_0 is significantly lower than for the semi-infinite layers they studied since energy loss of 20 kV electrons in the first 300 nm is relatively low. Finally, a discharge current $i(t)=-\frac{q}{RC}$ exits the nanowire to the tungsten tip. This current was measured by a picoampermeter that confirmed the positive charge. When illuminated the evolution of the nanowire charge is then given by

$$\frac{dq}{dt}=-q\left(\frac{1}{RC}+\frac{\delta_0 i_b}{Q_{max}}\right)+\delta_0 i_b, \tag{2}$$

which is governed by two time constants $\tau_1=RC$ and $\tau_2=Q_{max}/\delta_0 i_b$. In the following we assume $\tau_1 \ll \tau_2$ although self-sustained oscillations can be obtained in all cases. The electron beam is much smaller than the diameter ϕ and thus charging occurs when the nanowire center is within $\pm\phi/2$ of the focus point. Outside this interval the charge evolution is given by $\dot{q}=-q/RC$. The equations are coupled through the term $F(q)$ in Eq. (1) and dq/dt in Eq. (2).

Experimentally, when a charge q is localized on a nanowire it bends reproducibly in one direction (taken as $+x$) due to $F(q)$. This is particularly visible on highly insulating nanowires such as thin BN nanotubes and is governed by the capacitance. When no electrode is located in the vicinity of the nanowire, the asymmetry direction is controlled by the close environment, particularly the support tip and nanowire angle. Another electrode near the nanowire end, for example, a second tip intentionally displaced near the resonator, can override the support tip and nanowire asymmetry and define the direction of preferred motion. Formally $F(q)=-\frac{1}{2}\frac{\partial C}{\partial x}\frac{q^2}{C^2}$. Expressions for C [and $F(q)$] must be derived for each geometry. A complicated analytical expression for the capacitance and force was derived, valid when the nanowire and tungsten tip are far from other electrodes. For our nanowire this gives $C\simeq 10^{-15}$ F and $F(q)=aq^2$ with $a=10^{16}$ N C^{-2}. $F(q)$ can differ over orders of magnitude depending on the nanowire used but for the modelization presented here we found an averaged charge $\bar{q}\sim 10^{-14}$ C (see Fig. 2) and thus give an averaged force $F(q)\sim 10^{-12}$ N, a typical force for exciting nanoresonators. The resistivity of several of these nanowires has been determined to be $\simeq 100\ \Omega$ cm by field emission electron spectroscopy (see Ref. 11). This gives resistances of 10^{10}–$10^{12}\ \Omega$ for this nanowire.

These equations and parameters have been used to simulate the oscillations (see Figs. 2 and 3). In Fig. 2(a) the nanowire is initially immobile and the illumination starts at $t=0$. The movement starts with a nonoscillating deflection as the nanowire initially charges. Small amplitude oscillations begin when it exits from the beam. These grow during a tran-

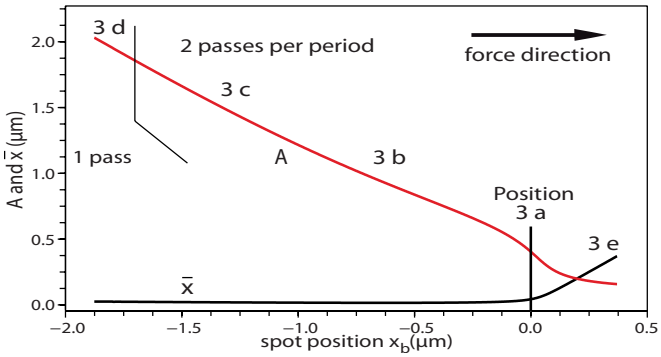

FIG. 3. (Color online) Results of the semianalytical calculations of the steady state parameters $\bar{x}$ and A for the nanowire motion as a function of the spot position with respect to the unperturbed nanowire position, x_b. The asymmetric response is very evident for the two parameters. Positions 3a–3e correspond to the scans in Fig. 1(d).

sient period before settling into a limit cycle of self-sustained oscillations. The position and velocity limit cycle is illustrated in the phase plane diagram in Fig. 2(b). After an initial increase, the position and charge stabilize around average values $\bar{x}$ and $\bar{q}$ with small oscillations. $\bar{x}$ is positive because of the average electrostatic forces on $\bar{q}$ which is the source of the asymmetrical behavior. Figure 2(d) shows a blowup of $x(t)$ and $q(t)$ (not to scale) when the limit cycle is reached. $x(t)$ is close to sinusoidal at the fundamental resonance frequency: $x(t) \approx \bar{x} + A\cos(\omega_0 t)$. This fact will be the basis of our analytical theory (see next paragraph). This figure illustrates the net energy injection. The light gray interval is when $F(q)$ removes energy $[F(q)\dot{x} < 0]$ and the dark gray interval is when $F(q)$ adds energy $[F(q)\dot{x} > 0]$. The small difference in $q(t)$ in these intervals [or $F(q)\dot{x}$] is responsible for the energy injection into the system that compensates the dissipative energy losses and permits the existence of a limit cycle.

Analytical forms for the steady state values of $\bar{x}$ and A can be obtained by charge and energy conservation. One assumes $x(t) = \bar{x} + A\cos(\omega_0 t)$, and integrates Eqs. (1) and (2) over a cycle. The analysis for motions with one or two passes per period must be examined separately. The existence and stability of the solutions for one pass will be presented elsewhere and here we discuss only the two pass motion. Experimentally we observed almost exclusively two passes per period except at the maximum x_b (where the two solutions are almost equivalent). The resulting explicit expressions are quite complicated but allow us to understand the notable experimental asymmetry as x_b is varied. Calculations are presented in Fig. 3. Note first that the steady-state oscillation for $x_b = 0$ has $\bar{x} > 0$ $[F(q) > 0]$. Displacing the spot in the $-x$ direction opposite to the $F(q)$ leads to a new equilibrium state with larger A and almost constant $\bar{x}$. The important increase in A is because the more the movement is asymmetric with respect to the irradiation zone (i.e., larger $\bar{x} - x_b$), the larger the energy injection.

As x_b is increased to the maximum $-x$ displacement (and maximum A), the time between passes eventually goes to zero and the solution becomes identical with the single pass solution. This position corresponds to the maximum energy injection into the system. The oscillations then abruptly disappear at still larger $-x$, i.e., no solution. This is precisely what is observed in experiment [Fig. 1(d), position d]. The behavior is radically different in the $+x$ direction. In this case we observe a rapid increase of $\bar{x}$ which tends to approach x_b (important increase $\bar{q}$) and the amplitude rapidly decreases (for charge conservation). This explains the enlargement of the peaks in Fig. 1(d), position e. In this case no solution exists with only one pass (in fact it would lead to negative energy injection).

Varying the parameters within reasonable ranges modifies quantitatively the nanowire motion but the general behavior and asymmetry are unchanged. For example, preliminary studies varying the electron beam (200–600 pA) and energy (15–25 kV) were carried out. Changing the current strongly affects the oscillation amplitude, while energy has a minor effect. However, both of these behaviors are well-described by the model. The palette of phase space trajectories and limit cycles is extremely rich, particularly in the transient period, with very different regimes delimited within specific parameter space windows. Among the many different possible parameter combinations, two time constants are of prime importance: $T = 1/\nu_0$ and RC. RC controls the charge loss and hence the equilibrium charge and position of the nanowire. If $RC \ll T$ the charge disappears between two consecutive irradiations and the nanowire charge receives a sudden kick at every pass. Even if the oscillation can still exist, the response includes higher harmonics. If $RC \gg T$ a large $\bar{q}$ tends to build resulting in large deflections and single passes. If not limited by the Q_{max}, the oscillating nanowire can then exit completely from the irradiation zone and the oscillations die off.

Measurements have been performed on numerous SiC nanowires of different dimensions. Only results for a large nanowire are presented in this first paper because it was easier to carry out systematic measurements. First this allowed easier microscopy imaging that suffered less from SEM beam-induced pollution. Second, the low resonance frequency allowed the use of the scintillator which has a relatively low frequency bandpass. The phenomenon is not restricted to such large nanowires, actually becoming more predominant for smaller nanowires. We carried out a limited number of measurements on several nanowires going down to 30 nm in diameter and 2 μm in length.

Self-sustained oscillations were originally achieved in only about half the samples because of the variable capacitive environment of the nanowire. If the resulting electrostatic force is not sufficient to cause the nanowire to make a first exit from the illumination zone, the excitation mechanism cannot start. To verify this hypothesis we modified the environment of the nanowire using a *xyz in situ* nanomanipulator that permits one to approach the nanowire with another tungsten tip as presented in Fig. 4. In this configuration the resulting electrostatic force should increase significantly. As expected when the second tip is close, all nanowires self-oscillate as in Fig. 1(d). Starting from this first position we displaced the nanowire symmetrically to the opposite side of the additional tip [Fig. 4(b)]. In this case the self-oscillations

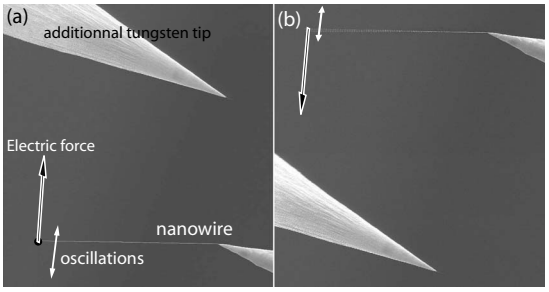

FIG. 4. Modification of the capacitive environment of the nanowire by approaching an additional tungsten tip with a *xyz in situ* manipulator on either side of the nanowire [images (a) and (b)]. The asymmetrical response as a function of spot position is described by the transversal double-headed arrows. The asymmetry changed sign as predicted for the two positions.

presented the opposite asymmetry as expected in the model. All these experiments clearly prove that these self-sustained oscillations are governed by the nanowire capacitance.

We performed complementary experiments in a transmission electron microscope. The same self-sustained oscillations were observed when the electron spot was concentrated on the nanowire. In this case excitation is achieved by placing it at the edge of the beam which is now much larger than the nanowire diameter. The gradient of beam intensity at the edge initiates the oscillations. Films of the excitation are presented in our web site.[12] The nanowire presented in the film has also been studied in SEM. It oscillated only when an additional tip was approached and its natural frequency was measured to be 21 kHz.

The self-sustained oscillations are often an undesired effect that can degrade image resolution and also could affect the interpretation of *in situ* vibration measurements. For thin and long nanowires we observed that small irradiation can cause the nanowire apex to stick the base tungsten tip. This work shows that these effects can be minimized by reducing the beam current and the capacitance by isolating the studied object.

In conclusion we have first shown that an electron beam provides a force for exciting self-sustained oscillations of a nanocantilever. These self-sustained oscillations can be used to rapidly determine the resonance frequency of individual nanowires, even within a mat-type sample or an integrated device structure, since it does not require an external excitation signal that is not always easy to apply. The spot mode is present in any SEM and thus this excitation technique can be used immediately by literally thousands of researchers in the world. Second we have developed a model which explains many of the details of the oscillation motion and its dependence on system parameters. An effort was made to use the real parameters of the nanowire environment. The simulations provide convincing evidence that the oscillations are due to the attraction of the beam induced charges on the nanowire to the environment. A final remark is that it is obvious that oscillations could be excited by directly modulating the electron beam.

This work opens perspectives in fundamental studies of nanocantilever excitation and detection, nanometric resonating devices such as the electron shuttle and low excitation-detection crosstalk. The focusing capabilities of electron microscopes means that this can be applied to the smallest cantilevers, in principle even single wall nanotubes, and thus lead to ultrasensitive measurements. It provides a parallel strategy to optical driving of NEMS where the charge force is a different mechanism than induced temperature variations. This mechanism is intimately related to the electrical properties of the system and thus in a very general way provides a model NEMS system in which the influence and interplay of the different parameters can be studied in a controlled way.

This work was carried out within the framework of the Group Nanowires-Nanotubes Lyonnais. The authors acknowledge the support of the "Plateforme Technologique de Microscopie" of Lyon. M. Choueib thanks the Lebanese CNRS for financial support.

*pascal.vincent@lpmcn.univ-lyon1.fr

[1] K. L. Ekinci and M. L. Roukes, Rev. Sci. Instrum. **76**, 061101 (2005).
[2] M. D. LaHaye, O. Buu, B. Camarota, and K. C. Schwab, Science **304**, 74 (2004).
[3] Y. T. Yang, C. Callegari, X. L. Feng, K. L. Ekincy, and M. L. Roukes, Nano Lett. **6**, 583 (2006).
[4] K. Aubin, M. Zalalutdinov, T. Alan, R. B. Reichenbach, R. Rand, A. Zehnder, J. Parpia, and H. Craighead, J. Microelectromech. Syst. **13**, 1018 (2004), and references therein.
[5] M. Bechelany, D. Cornu, F. Chassagneux, S. Bernard, and P. Miele, J. Optoelectron. Adv. Mater. **8**, 638 (2006); M. Bechelany, D. Cornu, and P. Miele, French Patent No. FR 2879627 (23 June 2006) and Patent No. WO 2006067308 (29 June 2006).
[6] P. Poncharal, Z. L. Wang, D. Ugarte, and W. A. de Heer, Science **283**, 1513 (1999).
[7] M. F. Yu, G. J. Wagner, R. S. Ruoff, and M. J. Dyer, Phys. Rev. B **66**, 073406 (2002).
[8] S. Perisanu, P. Vincent, A. Ayari, M. Choueib, M. Bechelany, D. Cornu, and S. T. Purcell, Appl. Phys. Lett. **90**, 043113 (2007).
[9] K. Kanaya and S. Okayama, J. Phys. D **5**, 43 (1972).
[10] T. Thome, D. Braga, G. Blaise, J. Cousty, L. Pham Vanand, and J. M. Constantini, Mater. Sci. Eng., B **130**, 177 (2006); T. Thome, D. Braga, and G. Blaise, J. Appl. Phys. **95**, 2619 (2004).
[11] S. T. Purcell, P. Vincent, C. Journet, and V. Thien Binh, Phys. Rev. Lett. **88**, 105502 (2002); S. T. Purcell, P. Vincent, M. Rodriguez, C. Journet, S. Vignoli, D. Guillot, and A. Ayari, Chem. Vap. Deposition **12**, 331 (2006).
[12] See website http://lpmcn.univ-lyon1.fr/~pvincent